Journal of Electrical and Computer Engineering Innovations
(JECEI)
Journal homepage: http://www.jecei.sru.ac.ir

Research paper

High-Performance and Efficient Induction Heating Circuit based on PCB Coils

Bahram Rashidi [*], ***Ali Mirzajani Nooshabadi***

Department of Electrical Engineering, Faculty of Engineering, Ayatollah Boroujerdi University, Boroujerd, Iran.

Article Info

Article History:
Received 13 May 2025
Reviewed 12 July 2025
Revised 10 August 2025
Accepted 30 August 2025

Keywords:
Induction heating
induction sealing
Induction PCB coils
Hardware implementation
Resonant converter

[*]Corresponding Author's Email Address: *b.rashidi@abru.ac.ir*

Abstract

Background and Objectives: This paper presents a high-performance and efficient circuit based on low-cost coils for induction heating applications. We design the coils specifically for induction sealing and induction cooker applications. The proposed circuit utilizes two parallel sets of MOSFET transistors to increase the current flow and output power.

Methods: Three types of coils have been developed in square and rectangular designs on the printed circuit board (PCB). In this case, the construction process is simple and requires minimal time. Induction coils designed for induction sealing applications have a rectangular structure that effectively seals a wide range of bottles.

Results: The flexibility of the proposed circuit is one of its advantages; the output frequency can be adjusted by increasing or decreasing the number of capacitors in the capacitor bank. Performance comparisons (e.g., efficiency, power density, cost) between the proposed method and other studies show that the implementation cost of the proposed circuit is lower than that of others. The proposed circuit achieves 95% efficiency. Thermal imaging confirms the circuit's performance. Based on the electromagnetic interference results, the circuit's performance is not affected by an external magnetic field.

Conclusion: The proposed circuit has been tested with different capacitor banks using two power supplies of 24 V and 12 V. The peak-to-peak output voltage is 181 V and 92 V for the 24 V and 12 V power supplies, respectively. The results demonstrate that the circuit and coils are suitable for induction heating applications.

How to cite this paper:
B. Rashidi, A. Mirzajani Nooshabadi, "High-performance and efficient induction heating circuit based on PCB coils," J. Electr. Comput. Eng. Innovations, 14(1): 197-210, 2026.
DOI: 10.22061/jecei.2025.11945.845
URL: https://jecei.sru.ac.ir/article_2411.html

Introduction

Induction heating is a technology with numerous advantages, including high efficiency, rapid heating, cleanliness, and precise control. Due to these benefits, this technology has become the preferred choice for industrial, domestic, and medical applications. This method offers a combination of speed, stability, and control for industrial applications. Advances in key technologies such as power electronics, control techniques, and magnetic device design have enabled the development of cost-effective and high-quality systems. Induction heating is accomplished by generating an oscillating signal with a frequency in the kHz range in an induction coil, which acts as the primary winding of a transformer. The metal to be heated serves as the secondary winding of the transformer, albeit short-circuited. When a piece of metal is placed near the inductor, rotating eddy currents are induced in the metal, generating heat. Induction heating, induction furnaces, and induction ovens are among the most important applications of induction heating, which have industrial (melting and shaping of metals), medical (sealing bottles of various medicines), and domestic (induction stoves for cooking) applications. For example, as a container containing medicine or a food item passes under an induction coil, eddy currents heat the aluminum foil in the container lid. The thin layer of polymer attached to the aluminum foil is melted, after cooling, the polymer sticks to the container and finally the product lid is sealed.

In recent years, studies [1]-[30] have discussed the design and implementation of induction heating circuits. For example, in [2], an oscillator circuit based on the second-order sliding mode control properties for air-cooled induction sealing is presented. In [3], the role of inverter topology in designing a 1.5 kW, 50 kHz induction sealing circuit is investigated. In [4], a planar litz structure in the PCB for the used chokes in domestic induction cookers is proposed. In [6], a high input power factor for industrial heating applications is achieved using a three-phase three-switch PWM rectifier. In [7], a method to investigate the current density of various Litz wire-based coils used in induction heating applications is presented. In [8], the current state of induction heating technology in industrial, domestic, and medical applications and the main milestones in the development of induction heating are analyzed. In [9], the authors presented a multi-zone induction heating circuit through a suitable spiral design. In [11], to design a sealing plastic microfluidic system, a low-frequency induction heating circuit is proposed. A self-resonant inverter for induction heating of melting furnaces based on parallel IGBTs is designed in [14]. In [15], the inductance of a flat air-core coil for induction heating applications based on an analytical calculation is achieved. In [16], induction heating systems whose coils are located significantly further from the load are studied. In [18], a finite element method (FEM) is used to design the induction coil during the heating period. In [21], the design and hardware implementation of an efficient and optimal induction heating circuit for induction sealing based on zero-voltage switching technology is presented. The induction coil has an elliptical structure using Litz wire. In [26] and [27], the salient features of converter topologies used for domestic and industrial heating applications with a focus on their stage-wise power conversion, power rating, power density, control range, modulation techniques, load handling capacity, soft switching, reliability and size are presented. In [30], a single-stage direct AC to high-frequency (HF) AC resonant converter based on LLC configuration for induction heating systems or HF applications is proposed.

This paper deals with the design of an effective circuit for induction heating applications. The proposed circuit has been tested and evaluated for different capacitor banks. The results show that the proposed circuit has an acceptable performance. The most important points of the proposed circuit design are as follows:

- A high-performance and efficient circuit based on low-cost coils for induction heating applications is presented, focusing on the design of coils for induction sealing and induction cooker applications.
- The proposed circuit is designed based on two sets of parallel transistors to increase the current flow and the output power of the circuit.
- In this paper, we have designed three types of coils in square and rectangular forms based on a printed circuit board (PCB). In this case, the construction process is simple and requires minimal time.
- One of the advantages of the proposed circuit is its flexibility, as the output frequency can be changed by increasing or decreasing the number of capacitors in the capacitor bank.

The remainder of this paper is organized as follows. First, an overview of induction heating is provided. Next, the proposed induction heating circuit architecture is described. Finally, the results and discussion are presented.

Induction Heating

One method of heating metals, such as aluminum, iron, and steel, is induction heating. In this method, without exposing the metals to an external heat source, the induction of a magnetic field creates an eddy current in the metal, causing it to heat up. In this case, the metal heats up faster. For example, in the sealing of bottles used in the food and pharmaceutical industries (the sealing of container lids helps establish product

credibility and durability), if direct heat is used, the plastic container deforms due to the high temperature. To prevent this, induction sealing is used, ensuring that only the aluminum foil in the lid is heated. The body of the container does not heat up, so only the aluminum is heated for sealing, and the heating of the aluminum melts the adhesive layer, completing the sealing process. This phenomenon is the most important and valuable feature of induction sealing. The highest current intensity is generated near the magnetic field. In this way, the aluminum foil in the bottle cap is heated and adheres to the container. The heating rate in induction heating depends on several factors, including the frequency and intensity of the induced current, the specific heat of the material, the material's magnetic permeability, and its electrical resistivity.

Fig. 1 shows two types of induction heating applications: (a) the induction sealing and (b) the induction cooker, respectively. The focus of this paper is the circuit design for induction sealing and induction heating. Fig. 1 (a) shows a bottle placed in the magnetic field around the coil (the bottle cap contains an aluminum layer and other layers necessary for sealing). This method allows containers to be sealed rapidly on a production line, significantly increasing packaging speed. In Fig. 1 (b), a metal container containing food is heated by being placed on an induction coil, and as the container heats up, the food inside also warms. One of the advantages of this method is that the container heats up much faster than traditional flame-based heating.

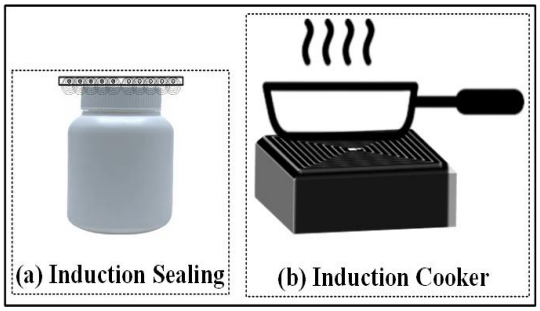

Fig. 1: The general structure of the induction sealing device with a bottle that is placed in the magnetic field around the coil (a), and the induction cooker (b).

The Proposed Structure of Induction Heating Circuit

The presented induction heating circuit operates using switching MOSFET transistors based on a zero-voltage switching technology. The switching frequency is determined by the capacitor bank's value and the output coil's inductance. When the transistors are switched on, they generate a high-frequency sinusoidal signal (in the kHz range) across the output coil, creating a surrounding magnetic field. This magnetic field results from the large current passing through the coil from the oscillator. The proposed circuit for induction heating is shown in Fig. 2. This circuit is used for various applications, such as induction sealing, induction cookers, and induction furnaces.

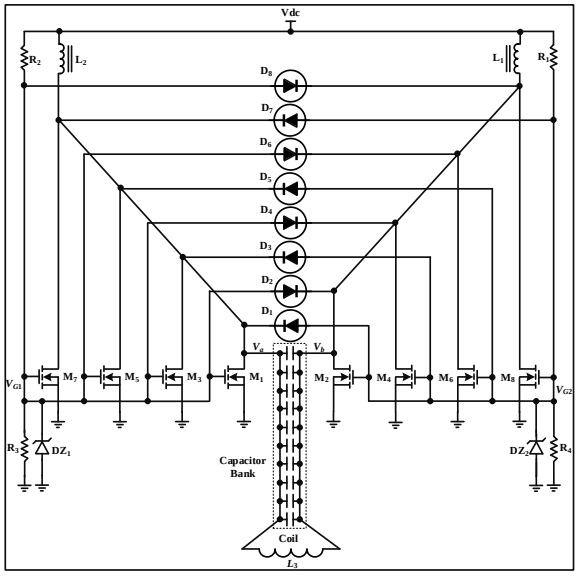

Fig. 2: The proposed circuit for implementation of the induction heating.

The parallel configuration of the transistors increases current flow and enhances the power transmitted to coil L_3. In each half-cycle of the output voltage, the transistors on one side of the circuit are on, and the current is divided between them. This arrangement improves the performance of the transistors. This circuit efficiently converts input DC voltage into high-frequency AC voltage at the output. The magnetic field generated around the output coil L_3 heats metal objects (such as iron and aluminum) by creating eddy currents. In this setup, eight MOSFETs (M_1 to M_8) are used to handle the required output current. To increase the power of the circuit, the transistors must have a high current-carrying capacity. In this case, the transistors must have a high current-carrying capacity. As we know, passing the rated current through a transistor causes it to overheat. In this circuit, to prevent this and increase the circuit's efficiency, we use parallel transistors. In this case, in each cycle, all the transistors on one side of the circuit are turned on and the current is divided between the transistors. This causes a current to pass through each transistor that does not cause it to overheat. In this case, by paralleling the transistors, we receive the maximum current from the power supply, and this increases the power at the output. In this circuit, each MOSFET transistor on the left side (M_1-M_3-M_5-M_7) is connected to its corresponding transistors on the right

side (M_2-M_4-M_6-M_8) via diodes (D_1-D_2, D_3-D_4, D_5-D_6, and D_7-D_8). In the proposed induction heating circuit, the gates of transistors M_1-M_3-M_5-M_7 are connected to the anodes of diodes D_2-D_4-D_6-D_8, as well as to the cathode of Zener diode DZ_1, resistors R_3-R_2, and one end of inductor L_1. A similar configuration exists for the transistors M_2-M_4-M_6-M_8 on the right side. On the other hand, the cathodes of diodes D_2-D_4-D_6-D_8 are connected to the drain pins of the corresponding transistors M_2-M_4-M_6-M_8. Zener diodes DZ_1 and DZ_2 protect the MOSFET gates by limiting their voltage and preventing potential damage. Resistors R_2-R_3 and R_4-R_1 are employed to control and trigger the MOSFET transistors. Fast diodes D_1 to D_8 facilitate rapid switching of the MOSFETs. Inductors L_1 and L_2 provide nearly constant current for the resonant circuit.

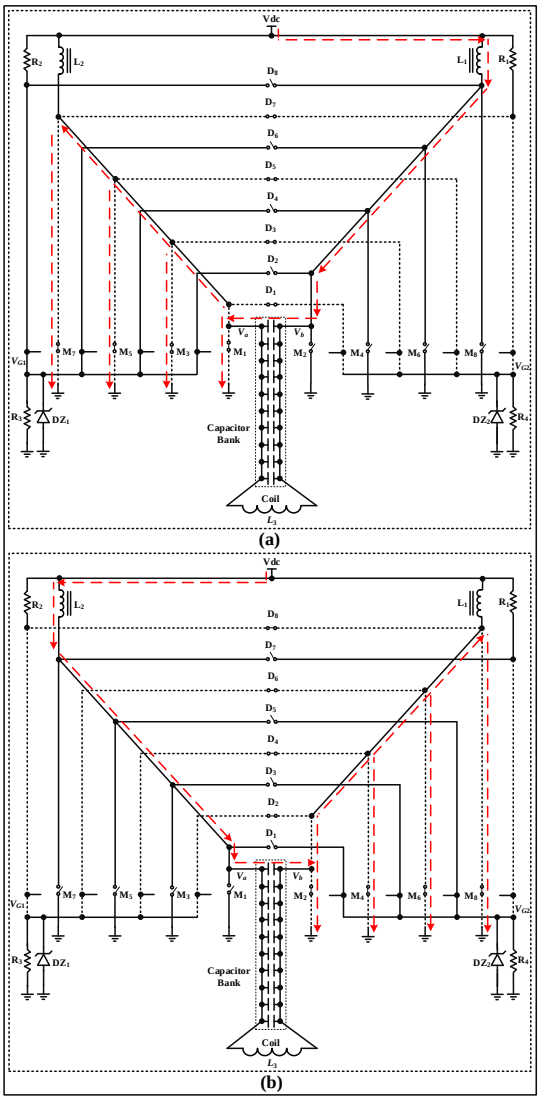

Fig. 3: The turning off and turning on process of the MOSFETs in the proposed circuit.

As the gate voltage of transistors M_1, M_3, M_5, and M_7 increases, these transistors turn on; their drain voltage decreases (to zero volts), and diodes D_1, D_3, D_5, and D_7 also turn on (Fig. 3 (a)). Turning on these diodes reduces the voltage (to zero) at the gates of transistors M_2, M_4, M_6, and M_8, turning these transistors off. In other words, when transistors M_1, M_3, M_5, and M_7 are on, transistors M_2, M_4, M_6, and M_8 are off. On the other hand, when the gate voltage of the transistors M_2, M_4, M_6, and M_8 increases, these transistors turn on, and diodes D_2, D_4, D_6, and D_8 also turn on (Fig. 3 (b)). Turning on these diodes reduces the voltage at the gates of transistors M_1, M_3, M_5, and M_7, turning these transistors off. The left and right transistors continue to cycle on and off, causing the circuit to oscillate at the resonant frequency of the $C_b - L_3$ circuit. C_b is the equivalent capacitance of parallel capacitors. The induction heating frequency is typically between 5 kHz and 70 kHz [7].

In this circuit, 10 capacitors are connected in parallel to the drains of the MOSFETs. The main coil of the induction heating circuit is connected to both ends of the capacitors.

The frequency of the circuit depends directly on the inductance of the coil L_3 and the capacitor equivalent of capacitor bank C_b. Oscillation frequency can be calculated using the following equation:

$$F = \frac{1}{2\pi\sqrt{L_3 C_b}} \tag{1}$$

In the following, based on the performance of the circuit, how to obtain (1) is described. Assume $I(t)$ is the instantaneous current flowing through the coil L_3. The voltage drop across the inductor is expressed in terms of current as $V_{L_3} = L_3 \frac{dI(t)}{dt}$ and the voltage drop across the capacitor bank is $V_{C_b} = \frac{Q}{C_b}$, where Q is the charge stored on the positive plate of the capacitor. According to Kirchhoff's voltage law, the sum of the potential drops across the components of a closed loop is equal to zero. Therefore, we can set up (2) for the closed loop containing and the capacitor:

$$V_{L_3} + V_{C_b} = 0 \tag{2}$$

Substituting the expressions for V_{L_3} and V_{C_b} gives us:

$$L_3 \frac{dI(t)}{dt} + \frac{Q}{C_b} = 0 \tag{3}$$

Dividing (3) by L_3 and derivative it with respect to parameter t, we have:

$$\frac{d^2 I(t)}{dt^2} + \frac{d}{dt}\frac{Q}{L_3 C_b} = 0 \longrightarrow \frac{d^2 I(t)}{dt^2} + \frac{1}{L_3 C_b}\frac{dQ}{dt} = 0$$

$$\xrightarrow{I(t)=\frac{dQ}{dt}} \frac{d^2 I(t)}{dt^2} + \frac{1}{L_3 C_b} I(t) = 0 \tag{4}$$

The Laplace transform of (4) is as follows:

$$s^2 + \omega^2 = 0, \tag{5}$$

Thus $s = \pm j\omega$, where j is the imaginary unit. The complete solution to the differential (5) is

$$I(t) = Ne^{+j\omega t} + Me^{-j\omega t}, \quad (6)$$

Since (6) involves complex exponentials, it represents a sinusoidal alternating current. However, because the electric current $I(t)$ is a physical quantity, it must be real-valued. Consequently, the constants N and M must be complex conjugates, such that $N = M^*$, Now let:

$$N = \frac{I_0}{2}e^{+j\phi}, M = \frac{I_0}{2}e^{-j\phi}, \quad (7)$$

Now the current in a simple harmonic oscillations form is given by:

$$I(t) = I_0 cos(\omega t + \phi), \quad (8)$$

where I_0 is the amplitude of the current, and ϕ is the phase angle. Put the value of (8) into (4) we get,

$$\frac{d^2I(t)}{dt^2} = -\frac{1}{L_3C_b}I(t)$$

$$\frac{d^2}{dt^2}I_0 cos(\omega t + \phi) = -\frac{1}{L_3C_b}I_0 cos(\omega t + \phi) \longrightarrow$$

$$\frac{d}{dt}[\frac{d}{dt}I_0 cos(\omega t + \phi)] = -\frac{1}{L_3C_b}I_0 cos(\omega t + \phi)$$

$$\frac{d}{dt}[-\omega I_0 sin(\omega t + \phi)] = -\frac{1}{L_3C_b}I_0 cos(\omega t + \phi) \longrightarrow$$

$$-\omega^2 I_0 cos(\omega t + \phi) = -\frac{1}{L_3C_b}I_0 cos(\omega t + \phi)$$

$$\omega^2 = \frac{1}{L_3C_b} \longrightarrow \omega = \omega_0 = \frac{1}{\sqrt{L_3C_b}} \quad (9)$$

Thus, from the (9), we can say that the L_3C_b circuit is oscillating and oscillates at a frequency called the resonant frequency. The induced voltage across an inductor is minus the voltage across the capacitor.

$$V = -L_3\frac{dI(t)}{dt} \quad (10)$$

Put the equation of current from (8), we get:

$$V(t) = -L_3\frac{d}{dt}[I_0 cos(\omega t + \phi)] \quad = -L_3I_0\frac{d}{dt}[cos(\omega t + \phi)]$$
$$= -L_3I_0[-\omega sin(\omega t + \phi)] \quad = \omega L_3I_0[sin(\omega t + \phi)] \quad (11)$$

(where, $\omega_0 = \frac{1}{\sqrt{L_3C_b}}$)

$$V(t) = \frac{1}{\sqrt{L_3C_b}}L_3I_0\sin(\omega t + \phi) = \sqrt{\frac{L_3}{C_b}}I_0\sin(\omega t + \phi) \quad (12)$$

The total impedance of the parallel L_3-C_b is given by

$$Z = \frac{Z_{L_3}Z_{C_b}}{Z_{L_3}+Z_{C_b}} \quad (13)$$

After substitution of $Z_{L_3} = j\omega L_3$ and $Z_{C_b} = \frac{1}{j\omega C_b}$ and simplification, gives

$$Z(\omega) = \frac{(j\omega L_3)(\frac{1}{j\omega C_b})}{j\omega L_3+\frac{1}{j\omega C_b}} = \frac{j\omega L_3}{-\omega^2L_3C_b+1} = -j\frac{\omega L_3}{\omega^2L_3C_b-1} \quad (14)$$

Using $\omega = \omega_0 = \frac{1}{\sqrt{L_3C_b}}$ it further simplifies to

$$Z(\omega) = -j\left(\frac{\frac{\omega l_3}{L_3C_b}}{\frac{\omega^2L_3C_b}{L_3C_b}-\frac{1}{L_3C_b}}\right) = -j(\frac{\frac{\omega}{C_b}}{\omega^2-\omega_0^2})$$

$$= \frac{j}{C_b}(\frac{\omega}{\omega_0^2-\omega^2}) = \frac{j}{C_b}(\frac{1}{\frac{\omega_0^2}{\omega}-\omega}) = \frac{j}{C_b\omega_0}(\frac{1}{\frac{\omega_0}{\omega}-\frac{\omega}{\omega_0}})$$

$$= \frac{j}{\frac{C_b\omega_0^2}{\omega_0}}(\frac{1}{\frac{\omega_0}{\omega}-\frac{\omega}{\omega_0}}) = \frac{j}{\frac{1}{L_3\omega_0}}(\frac{1}{\frac{\omega_0}{\omega}-\frac{\omega}{\omega_0}}) = j(\frac{\omega_0L_3}{\frac{\omega_0}{\omega}-\frac{\omega}{\omega_0}}) \quad (15)$$

According to the circuit, the value of $Z(\omega)$ at the resonant frequency must be infinite, that is:

$$(\lim Z(\omega))_{\omega\to\omega_0} = \infty \quad (16)$$

Note that for all other values of ω, the impedance $Z(\omega)$ is finite. Fig. 4 shows the waveforms of drain voltages V_a, V_b, gate voltages V_{G1}, V_{G2}, and the voltage waveform across the main coil L_3 (V_{ab}). It also briefly illustrates how transistors and diodes turn on and off according to the waveforms. As illustrated in Fig. 4, the drain voltage waveforms do not overlap, and the resulting output voltage V_{ab} exhibits a high-frequency sinusoidal shape.

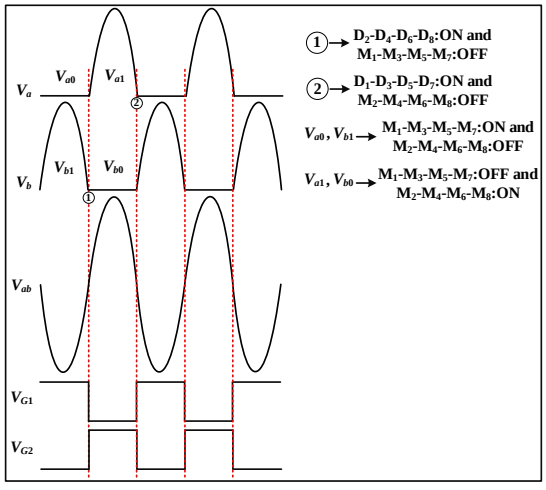

Fig. 4: The waveforms of drain voltages V_a, V_b, gate voltages V_{G1}, V_{G2}, and the voltage waveform across the main coil L_3 (V_{ab}).

A. Design of the Proposed Coils Based on PCB

In this paper, we have designed three types of coils

based on the printed circuit board (PCB) technology. Many previous works have utilized Litz wire and lacquer wire to fabricate coils (e.g., [7], [9], [16], and [21]). One of the challenges associated with these types of coils is the difficulty of their manufacturing process, as constructing circular (or square) and rectangular (or elliptical) coils using wire requires holding molds. In the proposed work, the coils are designed at the PCB level, simplifying and accelerating the construction process. Additionally, creating various designs (different shapes) at the PCB level is easier, and there is no restriction. Thus, we can fabricate coils on fiberglass substrates. Therefore, in this work, an induction coil at the PCB level is used to achieve performance comparable to traditional designs in terms of output power, efficiency, and thermal behavior. To enhance the current flow through the coil, we also apply additional tin to the PCB. The purpose of creating a coil at the PCB level is to design and manufacture a variety of coils in different shapes and sizes in the shortest possible time. Since the coils are implemented on the PCB surface, they do not have the problems of manufacturing coils made with lacquered wire.

In this case, the process of designing and manufacturing the coils occurs quickly. Also, coils with different shapes are easily manufactured. The only problem in the manufacturing process is re-tinning to increase the current flow of the coil paths.

Fig. 5 shows the proposed coils on the PCB surface for an induction heating circuit. The coils in Fig. 5 (a) and Fig. 5 (b) are suitable for induction sealing applications, while coil (c) is appropriate for an induction cooker. The coils in Fig. 5 (a) and Fig. 5 (b) generate a uniform magnetic field along their center.

This property is due to the wires being wound in a rectangular shape. In the rectangular coils, the long length produces a larger magnetic field per unit area. Thus, we have a magnetic field with a larger area. Due to the length of the coil, there is ample opportunity for the sealing action as the bottles pass along it. The coil in Fig. 5 (a) is suitable for bottles with a cap diameter greater than 10 cm. The coil shown in Fig. 5 (b) is suitable for bottles with a cap diameter smaller than 10 cm.

A uniform magnetic field along the length of the coil creates uniform heat in the aluminum foil and seals the bottle cap.

The amount of induction heat generated in the circuit can be controlled by changing the dimensions and number of turns of the coil, changing the width of the PCB track, and adjusting the current from the power source. The square coil shown in Fig. 5 (c) is suitable for an induction cooker, creating a concentrated magnetic field around itself.

The dimensions of the coils are shown in Fig. 5. The track width of the coils in Fig. 5 (a) and Fig. 5 (c) is 5 mm, while the track width in coil of Fig. 5 (b) is 2.5 mm. Rectangular coils need to be long enough so that the bottles on the conveyor have sufficient time to heat up, but for an induction cooker, a circular or square coil is a better choice.

Fig. 6 shows the magnetic field generated around the two coils. The field produced by magnetic induction can cause heating in metals such as aluminum, iron, and steel. As seen in Fig. 6 (a), there is a uniform field along the length of the coil that can create eddy currents across the entire surface of the aluminum foil. In this case, the sealing process is done using only one coil, eliminating the need for an additional coil. The creation of a uniform magnetic field along the length of the coil causes uniform heating of the aluminum foil on the bottle cap.

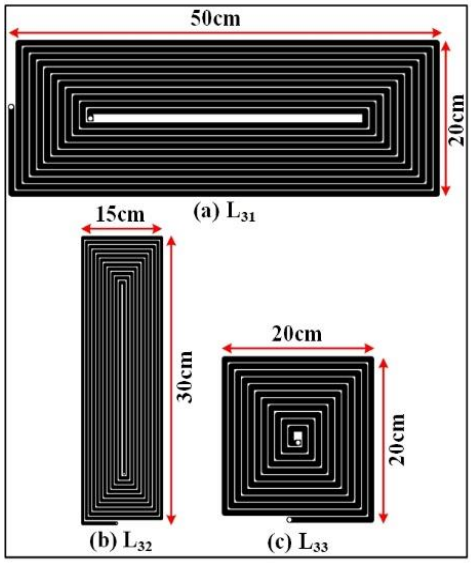

Fig. 5: The shape of the used coils in the induction heating circuit.

Fig. 6 (b) also generates a concentrated field at its center that can heat a pot of food.

The most important applications of induction heating circuits are induction cookers and induction sealing of pharmaceutical and food products.

Induction cookers mainly have circular or square coils, and induction sealing coils have elliptical or rectangular shapes.

In the present work, we use square and rectangular coils for induction cooker and induction sealing applications, respectively. Due to their square and rectangular structure, these types of coils are easier to implement on the PCB surface than circular and elliptical coils. According to the direction of current flow in the coil, a suitable field is created around it. This field is more in the center of the square coil and the rectangular coil.

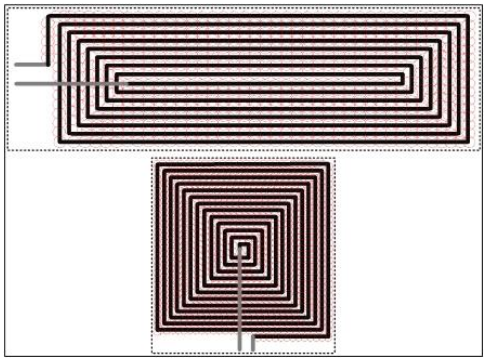

Fig. 6: Generated magnetic field around the coil.

B. Implementation of the Proposed Induction Heating Circuit

In this section, we will discuss the implementation of the presented circuit. The 470Ω resistances of R_1 and R_2 have a high current. To implement the R_1 and R_2 resistors, we use the equivalent resistors structure shown in Fig. 7. This configuration consists of four 470Ω 10W resistors connected in parallel (two by two), then two pairs of parallel resistors are connected in series. Thus, the equivalent resistance of these four resistors is equal to 470Ω. The current is divided among them, allowing the resistors to handle the high current more effectively. In other words, this configuration increases the power rating of the equivalent resistor, making it a more suitable replacement for a single 470Ω 10W resistor in circuit implementation.

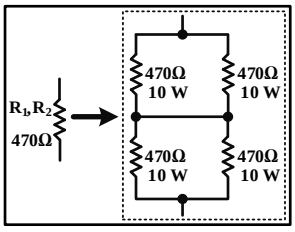

Fig. 7: The equivalent resistors to implement the R_1 and R_2 resistors.

Fig. 8 shows the hardware implementation of the three presented coils in Fig. 5. As mentioned before, the coil tracks are coated with additional tin to increase current flow and generate a strong magnetic field. The PCB for the induction heating circuit and its implementation are shown in Figs. 9 (a) and (b), respectively. The dimensions of this PCB are equal to 20cm×28cm. As shown in Fig. 9 (b), the tracks of the PCB are coated with additional tin to further increase current flow. The capacitor bank is constructed on a separate PCB. Finally, the implemented circuit based on 8 MOSFET transistors is shown in Fig. 10. In the proposed circuit, four MOSFET transistors are used on each side of the circuit to enhance current flow. This arrangement allows the current to be divided among the transistors. In this case, the cooling of the transistors becomes easier. The circuit is designed for applications that require higher output power.

Inductors L_1 and L_2 help to remove any high-frequency content from the power supply and limit the current to a safe level. These inductors have a ferrite core. In the implemented circuit, the inductors have an inductance of 100 μH with a current rating of 40 amps. The inner diameter of the inductors is 24 mm, the outer diameter is 47 mm, and the height is 18.2 mm. One of the advantages of this proposed circuit is its flexibility; by varying the number of capacitors in the capacitor bank, the output frequency can be adjusted. The capacitor bank is implemented separately, allowing for different banks to be used based on applications. The circuit can operate with power supplies ranging from 12V to 48V, depending on the application type. For industrial applications and sealing bottles with large cap diameters, a 24 V to 48 V power supply is appropriate, while a 12V supply is sufficient for low-power applications.

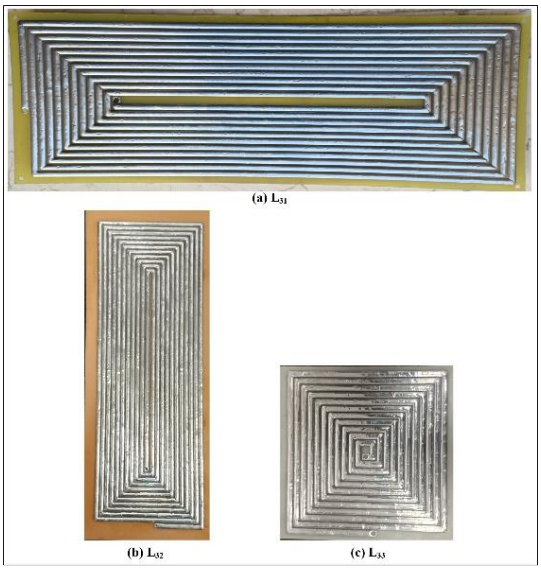

Fig. 8: The hardware implementation of the three used coils in the induction heating circuit.

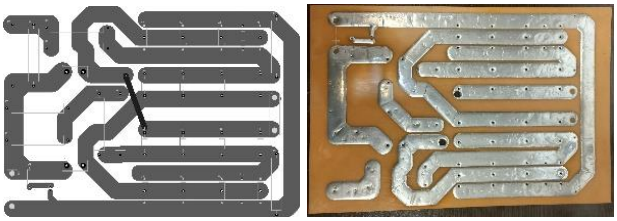

(a) (b)

Fig. 9: Printed circuit board of the induction heating circuit (a) and implementation of this board (b).

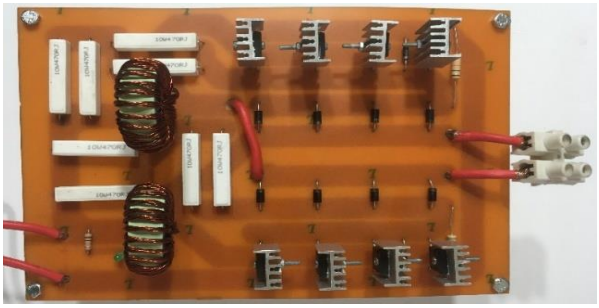

Fig. 10: The hardware implementation of the proposed induction heating circuit.

The main losses in this circuit occur in the transistors and the coil. To reduce the losses of the transistors, a heat sink and a fan are used. But for cooling the coil, several fans are also used above the coil. For industrial applications and for continuous use of the circuit, one of the important methods for cooling the coil is to use an oil-based cooling system. In this method, the coil is placed in a plastic box that has an oil inlet and outlet. The oil enters the box through the inlet and covers the coil, and the hot oil exits from the outlet. After this step, the oil enters a radiator equipped with a fan, and cooling occurs. A pump circulates the oil. In this cooling system, the circuit can work continuously.

Results and Discussion

This section presents the experimental results of the proposed induction heating system. The results are provided for two power supplies: 12 V (33 A) and 24 V (20 A). The specifications of the components used in the proposed circuit are summarized in Table 1. In this table, the inductance values of the coils L_{31}, L_{32}, and L_{33} are given.

Table 1: The specifications of the components used in the proposed circuit

Elements	Specification
R_1-R_2	470Ω, 10W
R_3-R_4	10kΩ, 5W
D_1-D_8	FR307
DZ_1-DZ_2	1N5349
M_1-M_8	IRFP260N
L_1-L_2	Toroidal inductor 100uH, 40A
Coils L_{31}-L_{32}-L_{33}	32.226µH-17.511µH-10.848µH

Tables 2 and 3 show the output signal characteristics at both ends of the coils and the current received from the input power supply for the different capacitor banks. These tables present the peak-to-peak output voltage, the DC current from the power supply, and the output frequency. In this study, we use three capacitor banks of 1.5μF (10 capacitors of 150nF, 630V), 3.3μF (10 capacitors of 330nF, 630V), and 5.98μF (4 capacitors of 1μF, 630V and 6 capacitors of 330nF, 630V). Since the inductance of the coil is constant, we can change the value of the capacitor bank to reduce and increase the output frequency. In this case, we create different capacitor banks according to the application, and by changing the capacitor bank, the desired frequency can be achieved. Fig. 11 shows a type of variable capacitor bank configuration. In this structure, by connecting and disconnecting the switches, the number of parallel capacitors can be increased or decreased. By doing this, the equivalent capacitance of the capacitor bank can be changed without replacing the entire capacitor bank, allowing the desired frequency to be reached using only the switches. To increase the output frequency, a large number of capacitors can be placed in the capacitor bank. By using capacitors with small capacitance, the desired frequency can be reached more accurately.

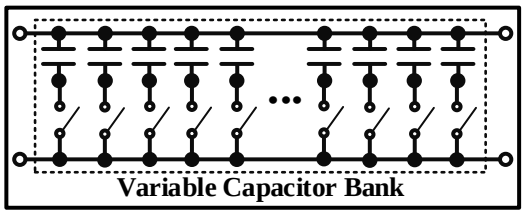

Fig. 11: A type of variable capacitor bank configuration for the proposed induction heating circuit.

For the experiments, a 6cm×6cm aluminum sheet was used to test the coils (by bringing it close to the coil). The results indicate that the circuit with a 24V power supply yields better results than the one with a 12V power supply. The 24 V power supply provides a higher heating rate and amount of heat in the aluminum sheet. The achieved temperature is adequate for effective sealing operations.

Table 2: Output voltage of the coils L_{31}, L_{32}, and L_{33} for different capacitance banks and the input DC voltage of 24V

Case	V_{ab}P-P(v)	I_{dc}	Freq.(kHz)
L_{31}, C_b=1.5µF	181	2.41	24.03
L_{31}, C_b=3.3µF	181	3.93	16.44
L_{31}, C_b=5.98µF	181	6.4	12.01
L_{32}, C_b=1.5µF	181	6.54	31.44
L_{32}, C_b=3.3µF	181	13.38	21.36
L_{32}, C_b=5.98µF	181	18.73	15.72
L_{33}, C_b=1.5µF	181	8.71	40.65
L_{33}, C_b=3.3µF	181	12.1	27.47
L_{33}, C_b=5.98µF	181	16.7	20.40

Table 3: Output voltage of the coils L_{31}, L_{32}, and L_{33} for different capacitance banks and the input DC voltage of 12V

Case	V_{ab} P-P(v)	I_{dc}	Freq.(kHz)
L_{31}, C_b=1.5µF	92	1.4	23.69
L_{31}, C_b=3.3µF	92	2.88	16.44
L_{31}, C_b=5.98µF	92	4.14	12.01
L_{32}, C_b=1.5µF	92	4.8	30.12
L_{32}, C_b=3.3µF	92	6.61	20.92
L_{32}, C_b=5.98µF	92	0.46	15.43
L_{33}, C_b=1.5µF	92	9.03	39.16
L_{33}, C_b=3.3µF	92	10.55	27.02
L_{33}, C_b=5.98µF	92	1.41	20.01

The waveforms corresponding to the two coil ends, gate voltage V_{G1}, and gate voltage V_{G2} for the three coils L_{31}, L_{32}, and L_{33} of the capacitor bank C_b = 3.3μF are shown in Fig. 11, Fig. 12, and Fig. 13, respectively. The figures were achieved by the oscilloscope with a 24 V power supply.

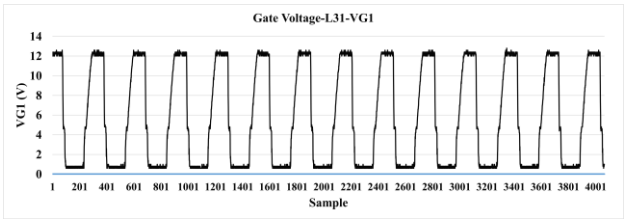

(a)

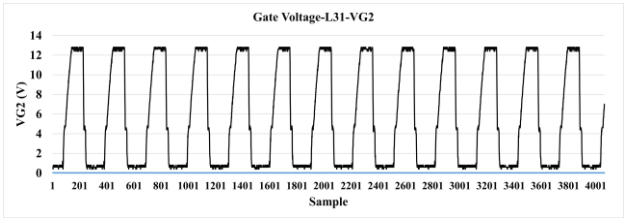

(b)

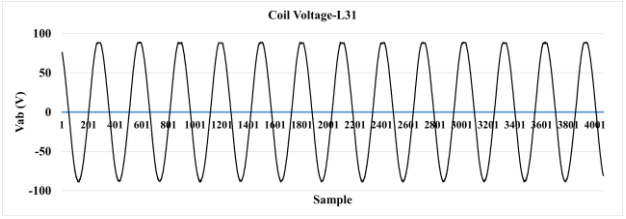

(c)

Fig. 11: The gate voltage V_{G1} of the MOSFETs (a), the gate voltage V_{G2} of the MOSFETs (b), and the output voltage of the coil V_{ab} (L_{31}) F=16.44kHz (c) in the oscilloscope for capacitor bank C_b=3.3μF.

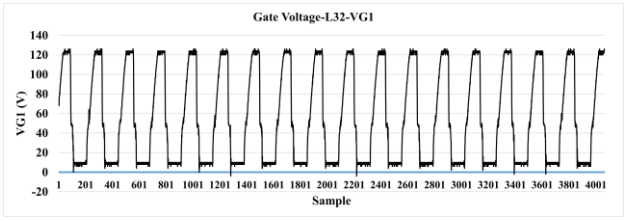

(a)

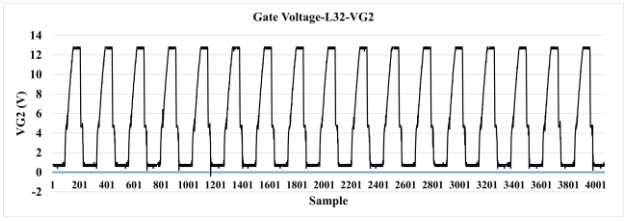

(b)

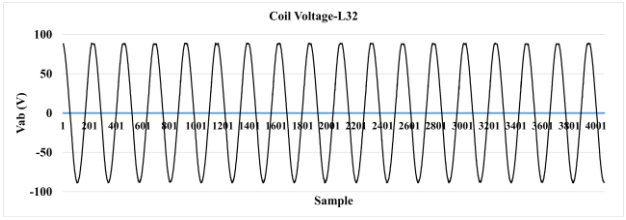

(c)

Fig. 12: The gate voltage V_{G1} of the MOSFETs (a), the gate voltage V_{G2} of the MOSFETs (b), and the output voltage of the coil V_{ab} (L_{32}) F=21.36kHz (c) in the oscilloscope for capacitor bank C_b=3.3μF.

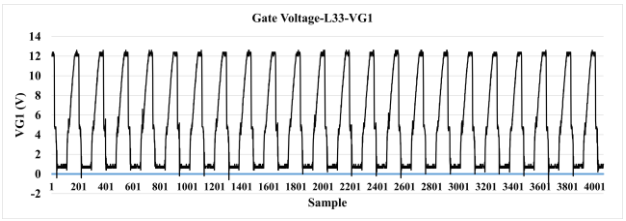

(a)

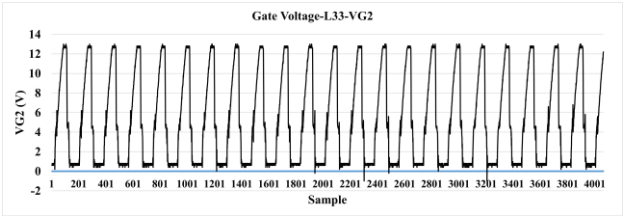

(b)

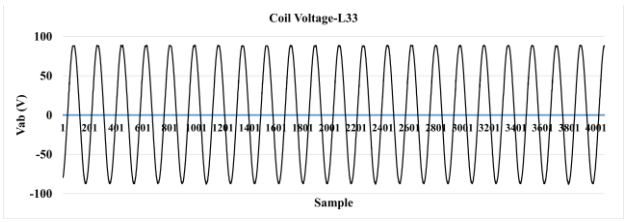

(c)

Fig. 13: The gate voltage V_{G1} of the MOSFETs (a), the gate voltage V_{G2} of the MOSFETs (b), and the output voltage of the coil V_{ab} (L_{33}) F=27.47kHz (c) in the oscilloscope for capacitor bank C_b=3.3μF.

As can be seen in these figures, based on the inductance values of coils L_{31}, L_{32}, and L_{33} (as presented in Table 1), the circuit with coil L_{33} has the highest frequency. The gate voltages are in pulse form; when V_{G1} is on, V_{G2} is off, which indicates that when the transistors on the right side are on, the transistors on the left side are off. As previously mentioned, the output voltages are sinusoidal and have achieved the desired frequency, consistent with the inductance values of the coils and the capacitance of the capacitor bank. These results indicate that the proposed circuit performs effectively in generating the desired output.

Performance comparisons (e.g., efficiency, power density, cost) of the proposed method and other works are shown in Table 4. The cost of the implementation of the proposed circuit is lower than that of the other works.

Table 4: Performance comparison of the proposed method and other works

Works	V_{out}(V)	Power(W)	Efficiency	Cost
[9] 4-coil	39	207	---	High
[9] 6-coil	54	290	---	High
[16]	---	3700	96 %	High
[19]	58	3000	96 %	High
[23]	---	800	94.26 %	High
[30]	88	1100	93 %	High
This work L_{31}	90	500	95 %	Low
This work L_{32}	90	500	95 %	Low
This work L_{33}	90	500	95 %	Low

Examples of sealed bottles with the coils L_{32} and L_{31} and boiling water with coil L_{33} are shown in Fig. 14. The diameters of the bottles are equal to 4 cm and 13 cm, which are commonly used in the pharmaceutical industry. The sealing performed by the coils and the proposed circuit has acceptable results. Additionally, the water in the aluminum container reached the boiling point quickly when heated by the coil L_{33}.

Thermal images of the coils were captured during operation under various load conditions using the AMG8833 thermal camera sensor module. For example, Figs. 15 and 16 (a)-(c) show thermal images of three aluminum foils with sizes of 3cm*3cm, 5cm*5cm, and 7cm*7cm, for maximum range of 40 °C and 80 °C, respectively, by the coil L_{33}. As can be seen, based on the temperature distribution, the foils have a high temperature compared with other areas. The highest temperature is generated in the center of the coil, indicating normal circuit operation.

Fig. 14: Examples of sealed bottles with the coils L_{32} and L_{31} and boiling water with coil L_{33}.

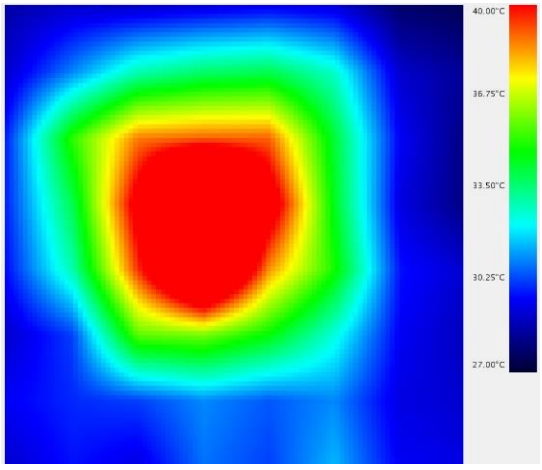

(a)

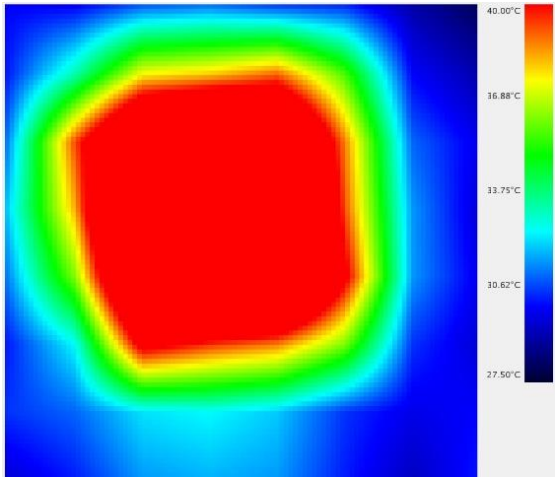

(b)

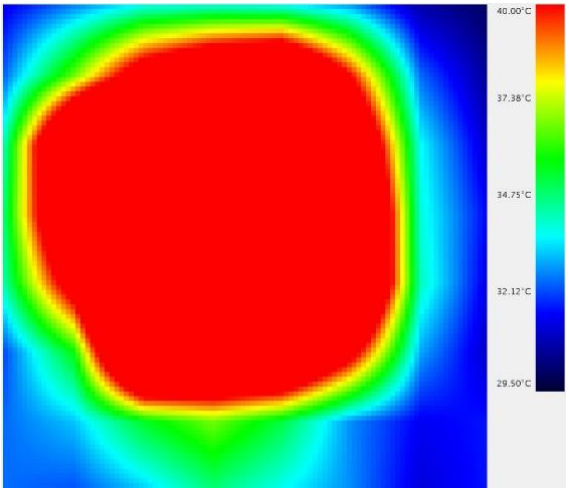

(c)

Fig. 15: Thermal images of three aluminum foils with sizes of 3cm*3cm (a), 5cm*5cm (b), and 7cm*7cm (c) by the coil L_{33} for maximum range of 40 °C.

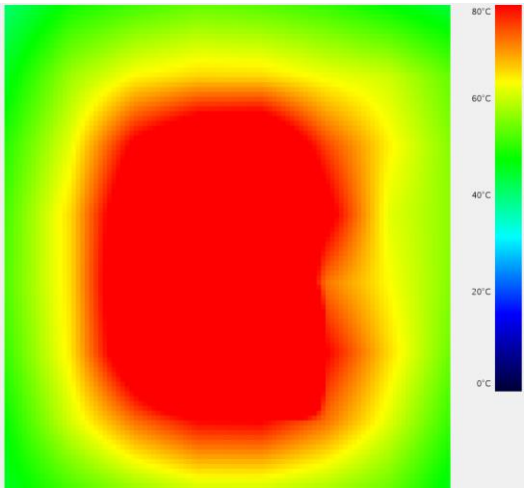

(c)

Fig. 16: Thermal images of three aluminum foils with sizes of 3cm*3cm (a), 5cm*5cm (b), and 7cm*7cm (c) by the coil L_{33} for maximum range of 80 °C.

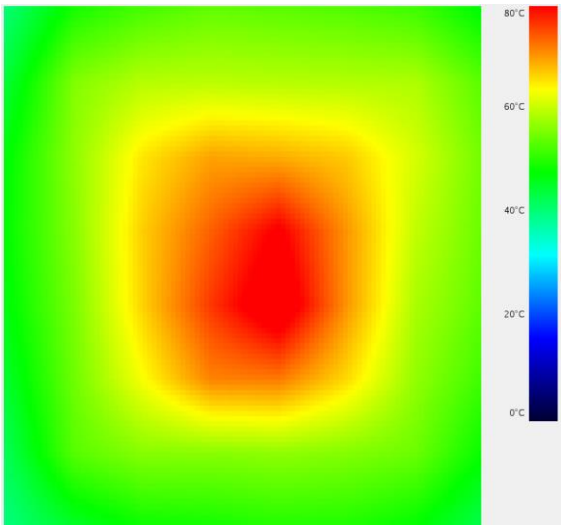

(a)

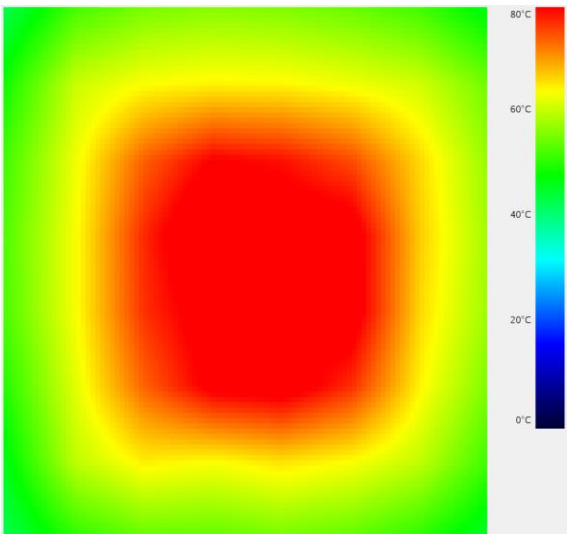

(b)

Thermal rise times for the coils L_{32} and L_{33} for different capacitance banks, different foil sizes, and the input DC voltage of 24V are presented in Table 5.

The times are measured in seconds. In this measurement, the target temperature is equal to 75 °C. As can be seen, the heating time decreases as the capacitance of the capacitor bank and the dimensions of the foil increase.

Table 5: Thermal rise times for the coils L_{32} and L_{33} for different capacitance banks, different foil sizes, and the input DC voltage of 24V

Case	Foil 3cm*3cm	Foil 5cm*5cm	Foil 7cm*7cm
L_{32}, C_b=1.5µF	53.41	47.26	40.20
L_{32}, C_b=3.3µF	32.80	30.55	23.88
L_{32}, C_b=5.98µF	18.05	16.94	8.53
L_{33}, C_b=1.5µF	45.62	42.31	18.46
L_{33}, C_b=3.3µF	29.17	14.05	6.08
L_{33}, C_b=5.98µF	18.69	7.15	4.20

The times are measured in seconds. The target temperature is equal to 75 °C.

A. Impact of EMI/EMC on System Performance

In recent years, the significance of electromagnetic interference (EMI) and electromagnetic compatibility (EMC) has become increasingly critical in the development of high-frequency technologies. As these devices are integrated into a diverse array of

environments, ensuring that they do not generate excessive electromagnetic noise while maintaining reliable performance is essential. This challenge is particularly relevant as it directly impacts the functionality and safety of interconnected electronic systems.

Therefore, a thorough investigation of EMI and EMC is not only necessary for compliance with established standards but also vital for the practical application and acceptance of our proposed technology.

The strategies for dealing with electromagnetic interference and improving electromagnetic compatibility:

1. **Shielding**: Using metallic covers or specialized materials to prevent EMI from entering or exiting a device. These shields can be applied to the design of device enclosures or specific modules. The shielding of the proposed circuit can be a useful approach.
2. **Filtering**: Installing EMI filters at the inputs and outputs of a system to reduce electromagnetic interference in electrical signals.
3. **Optimized Circuit Design**: Reducing the length of transmission lines, utilizing differential circuits, and proper PCB design can help mitigate EMI.
4. **Grounding Systems**: Implementing proper grounding designs to minimize noise and interference. Using a suitable grounding for the proposed circuit is a helpful method for dealing with EMI and EMC.

For this purpose, we have performed various tests by applying a magnetic field using a Helmholtz coil, which shows that the circuit is not affected by external fields and magnetic disturbances.

A Helmholtz coil generates a uniform magnetic field. The diameter of the Helmholtz coil is 44 cm. The distance between the pairs is 22 cm. Each coil has 37 turns of copper wire.

The alternating current in the coil is 1.7A to produce a uniform alternating magnetic field of 257uT (magnetic flux density) at 50 Hz.

The coils are placed in the middle of the Helmholtz pair. Fig. 17 shows the test setup for applying the external magnetic field.

In this case, we have placed the circuit in an external magnetic field and studied the performance of the circuit.

According to the results obtained, the performance of the circuit is not disturbed by applying an external magnetic field.

Fig. 17: Test setup for applying the external magnetic field.

Conclusion

In this paper, we presented a high-performance and efficient induction heating circuit based on low-cost coils. The proposed circuit operates as a converter, converting a DC voltage into an AC voltage at the output coil with the proper frequency. It is designed using two sets of parallel transistors to enhance current flow and increase the output power.

We have designed three types of coils in the form of square and rectangular configurations based on the PCB. This approach simplifies the construction process and requires minimal time.

The coils are designed for use in both induction sealing—capable of sealing a wide variety of bottle sizes—and induction cooking applications. The output frequency can be adjusted by varying the number of capacitors in the capacitor bank.

This feature makes the circuit flexible. The circuit's performance was tested for sealing various bottles and boiling water in an aluminum container, which confirmed the circuit's performance.

Author Contributions

Conceptualization and design, B. Rashidi; writing-original draft preparation, B. Rashidi; Hardware implementation, B. Rashidi and A. Mirzajani; Interpretation of the results and writing of the manuscript, B. Rashidi.

Acknowledgment

The authors would like to thank the reviewers for their comments. The authors have not received any financial support from any organization concerning this research.

Funding

This research received no external funding.

Conflict of Interest

The authors declare no potential conflict of interest regarding the publication of this work.

Abbreviations

PCB	Printed Circuit Board
FEM	Finite Element Method
HF	High-Frequency
EMI	Electromagnetic Interference
EMC	Electromagnetic Compatibility

References

[1] A. Sherwali, W. Dunford, "Experimental evaluation of heating water by electromagnetic induction," in Proc. the IEEE Canadian Conference of Electrical and Computer Engineering (CCECE): 1-4, 2019.

[2] A. Kumar Paul, "Robust features of SOSMC guides in quality characterization of tank circuit in air-cooled induction cap sealing," IEEE Trans. Ind. Appl., 54(1): 755-763, 2018.

[3] A. Kumar Paul, "Inverter topology for zero-ventilated high frequency induction heating systems," in Proc. the IEEE International Conference on Power Electronics, Drives and Energy Systems (PEDES): 1-6, 2020.

[4] I. Lope, J. Acero, J., Burdio, C. Carretero, R. Alonso, "Design and implementation of PCB inductors with litz-wire structure for conventional-size large-signal domestic induction heating applications," IEEE Trans. Ind. Appl., 51(3): 2434-2442, 2014.

[5] F. D. Marques, M. N. Souza, F. G. Souza, "Sealing system activated by magnetic induction polymerization," J. Appl. Polym. Sci., 134(47): 1-9, 2017.

[6] T. Ngo-Phi, N. Nguyen-Quang, "Variable pulse density modulation for induction heating," in Proc. International Symposium on Electrical and Electronics Engineering (ISEE): 1-6, 2012.

[7] A. Kumar Paul, "Current density characterization of litz wires used in induction heating coils: A practical approach," in Proc. the IEEE International Conference on Power Electronics, Drives and Energy Systems (PEDES): 1-6, 2018.

[8] O. Lucia, P. Maussion, E. Dede, J. Burdio, "Induction heating technology and its applications: Past developments, current technology, and future challenges," IEEE Trans. Ind. Electron., 61(5): 2509-2520, 2014.

[9] A. Kumar Paul, S. Chinoy, "Air cooled induction heater for efficient sealing of containers using wide range foils," IEEE Trans. Ind. Appl., 52(4): 3398-3407, 2016.

[10] A. Kumar Paul, "Structured protection measures for better use of nanocrystalline cores in air-cooled medium-frequency transformer for induction heating," IEEE Trans. Ind. Electron., 68(5): 3898-3905, 2021.

[11] B. Knauf, D. P. Webb, C. Liu, P. P. Conway, "Low frequency induction heating for the sealing of plastic microfluidic systems," J. Microfluid. Nanofluid., 9: 243-252, 2010.

[12] A. Kumar Paul, "ZVZCS SRI guides optimal use of copper and core for air-cooled nanocrystalline transformer for induction heating," IEEE Trans. Ind. Appl., 56(2): 970-978, 2020.

[13] R. Goldstein, W. Stuehr, M. Black, "Design and fabrication of inductors for induction heat treating," J. Neural Eng. 2014, Book chapter, ASM Handbook, 4(16): 589-606, 2014.

[14] B. Dimitrov, K. Hayatleh, S. Barker, G. Collier, "Design, analysis and experimental verification of the self-resonant inverter for induction heating crucible melting furnace based on IGBTs connected in parallel," Electricity, 2: 439-458, 2021.

[15] I. Hussain, D. K. Woo, "Inductance calculation of single-layer planar spiral coil," Electronics, 11: 1-10, 2022.

[16] E. Plumed, J. Acero, L. Lope, J. Burdio, "Design methodology of high-performance domestic induction heating systems under worktop," IET Power Electron., 13(2): 300-306, 2020.

[17] T. Pandey, P. Deo, A. Dongriyal, B. Patil, "Development of induction sealer and its application in food packaging," Int. Adv. Res. J. Sci. Eng. Technol., 7(3): 16-23, 2020.

[18] I. M. Abdulbaqi, A. H. A. Kadhim, A. H. Abdul-Jabbar, F. A. Abood, T. K. Hasan, "Design and implementation of an induction furnace, Diyala J. Eng. Sci., 08(01): 64-82, 2015.

[19] N. Vilchez, M. O. Varela de Seijas, A. Bardenhagen, T. Rohr, E. Stoll, "A novel induction heater for sintering metal compacts with a hybrid material extrusion device," Electronics, 12: 1-23, 2023.

[20] J. Serrano, J. Acero, I. Lope, et al., "A flexible cooking zone composed of partially overlapped inductors," IEEE Trans. Ind. Electron., 65(10): 7762-7771, 2018.

[21] B. Rashidi, "Hardware structure of an efficient and optimal circuit for induction cap sealing," Int. J. Ind. Electron. Control Optim., 7(3): 203-212, 2024.

[22] I. Sheikhian, N. Kaminski, S. Vob, W. Scholz, E. Herweg, " Optimisation of the reverse conducting IGBT for zero-voltage switching applications such as induction cookers," IET Circuits Devices Syst., 8(3): 176 -181, 2014.

[23] E. Jang, M. Jae Kwon, S. Min Park, H. Min Ahn, B. Kuk Lee, "Analysis and design of flexible-surface induction-heating cooktop with GaN-HEMT-based multiple inverter system," IEEE Trans. Power Electron., 37(10): 12865- 12876, 2022.

[24] J. Villa, D. Navarro, A. Dominguez, J. I. Artigas, L. A. Barragan, "Vessel recognition in induction heating appliances-a deep-learning approach," IEEE Access, 9: 16053-16061, 2021.

[25] F. Schapiro, "Using dynamic thermal imaging to correct sealing problems," Pharm. Technol., 39(11): 50-51, 2015.

[26] P. Vishnuram, G. Ramachandiran, S. Ramasamy, D. Dayalan, "A comprehensive overview of power converter topologies for induction heating applications," Int. Trans. Electr. Energ. Syst., 30: 1-33, 2020.

[27] P. Vishnuram, G. Ramachandiran, T. Sudhakar Babu, B. Nastasi, "Induction heating in domestic cooking and industrial melting applications: A systematic review on modelling, converter topologies and control schemes," Energies, 14(20): 1-34, 2021.

[28] V. Jagannath Patil, A. M. Mulla, "A critical review on the low power SIC MOSFET based current fed inverter used in surface hardening application," in Proc. 3rd International Conference on Electronics and Sustainable Communication Systems (ICESC): 1-6, 2022.

[29] K. Sayed, F. Abo-Elyousr, F. N. Abdelbar, H. El-Zohri, "Development of series resonant inverters for induction heating applications," Eur. J. Eng. Res. Sci., 3(12): 36-39, 2018.

[30] A. Kumar, A. Goswami, P. Kumar Sadhu, J. R. Szymanski, "Single-stage LLC resonant converter for induction heating system with improved power quality," Electricity, 5: 211-226, 2024.

Biographies

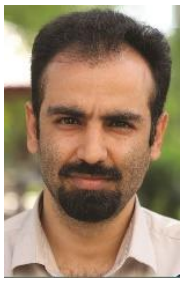

Bahram Rashidi was born in Boroujerd, Iran, in 1986. He received his B.Sc. degree in Electrical Engineering from Lorestan University, Iran, in 2009. He received his M.Sc. from Tabriz University, Iran in 2011 and he obtained his Ph.D degree from Isfahan University of Technology (IUT), in 2016, where he is currently an associate professor in the department of Electrical Engineering at Ayatollah Boroujerdi University. His research interests include industrial electronics, hardware implementation for the arithmetic of finite fields, cryptographic hardware, Block ciphers and VLSI circuits for elliptic curve cryptosystems.

- Email: b.rashidi@abru.ac.ir
- ORCID: 0000-0001-9662-3197
- Web of Science Researcher ID: ACQ-5592-2022
- Scopus Author ID: 54884845500
- Homepage: https://abru.ac.ir/users/bahram-rashidi/fa/

Ali Mirzajani Nooshabadi was born in Kashan, Iran, in 2003. He is a bachelor's student in the department of Electrical engineering at Ayatollah Boroujerdi University, Iran. His research interests include industrial electronics and hardware implementation.

- Email: stu.ali.mirzajani@abru.ac.ir
- ORCID: 0009-0007-5153-2524
- Web of Science Researcher ID: NA
- Scopus Author ID: NA
- Homepage: NA